

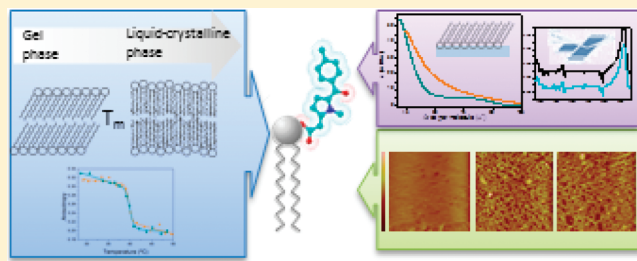
Lipid–Drug Interaction: Biophysical Effects of Tolmetin on Membrane Mimetic Systems of Different Dimensionality

Cláudia Nunes,[†] Gerald Brezesinski,[‡] Daniela Lopes,[†] José L.F.C. Lima,[†] Salette Reis,[†] and Marlene Lúcio^{*†}

[†]REQUIMTE, Departamento de Química, Faculdade de Farmácia, Universidade do Porto, 164, Rua Aníbal Cunha, Porto, Portugal

[‡]Max Planck Institute of Colloids and Interfaces, Science Park Golm, Am Mühlenberg 1, D-14476 Potsdam, Germany

ABSTRACT: This work focuses on the application of different biophysical techniques to study the interaction of tolmetin with membrane mimetic models of different dimensionality (liposomes, monolayers, and supported lipid bilayers) composed of 1,2-dipalmitoyl-*sn*-glycero-3-phosphocholine (DPPC), used as a representative phospholipid of natural membranes. Several biophysical techniques were employed: Fluorescence steady-state anisotropy to study the effects of NSAIDs on membrane microviscosity and thus to assess the main phase transition of DPPC, surface pressure-area isotherms to evaluate the adsorption and/or penetration of NSAIDs into the membrane, IRRAS to acquire structural information of the lipid membrane upon interaction with the drugs, and AFM to study the dynamic change in surface topography of the lipid bilayers caused by interaction with tolmetin. The experiments were performed taking into account the physiological conditions that tolmetin may find in the course of its *in vivo* therapeutic activity. Therefore, the studies covered the interactions of tolmetin with lipid membranes in both gel and liquid-crystalline phases at two pH conditions: 7.4 (plasma pH) and 5 (inflamed tissue pH). The applied models and techniques provided detailed information about different aspects of the tolmetin-membrane interaction. The studies have shown that tolmetin-membrane interaction is strongly dependent on the degree of drug ionization and of the lipid phase state, which can be related with the therapeutic action and gastro intestinal toxicity of this drug.



INTRODUCTION

Tolmetin, a nonsteroidal anti-inflammatory drug (NSAID), is a pyrrole acetic acid derivative¹ (Figure 1) with anti-inflammatory, analgesic, and antipyretic activity.² Tolmetin is effective both in treating the acute flares and in the long term management of the symptoms of several muscle skeletal diseases, such as rheumatoid arthritis and osteoarthritis.²

Inhibition of the membrane associated enzyme cyclo-oxygenase (COX) is the central mechanism by which NSAIDs reduce inflammation. Tolmetin is nonselective to the inducible COX-2 and inhibits the constitutive COX-1 causing the depletion of prostaglandins that are responsible for both inflammation and protection of the gastrointestinal (GI) tract.² Furthermore, tolmetin partitions into the cell membrane and is able to pass through the membrane lipid bilayer by passive transmembrane diffusion, being almost completely absorbed in the GI tract.² The enhanced GI absorption can result in a chemical association between tolmetin and GI membrane phospholipids compromising the integrity of the GI mucosa.² Consequently, both the nonselectivity of tolmetin toward COX-2 and the local effect of tolmetin in GI lipid membranes may partially explain the GI toxicity of this drug, which can cause serious adverse events including bleeding, ulceration, and perforation of the stomach or intestines.²

Tolmetin is also associated with an increased risk of cardiovascular thrombotic events, myocardial infarction and stroke.² These pathologies may as well be related with alterations in

membrane lipid composition and structure³ that arise from drug-membrane interactions.

Apart from the toxic GI and cardiovascular effects of tolmetin, it has been reported that this NSAID possesses antioxidant properties.⁴ Once again, the interplay between tolmetin and membrane lipids might be related with the antioxidant efficiency of this drug, as it has been suggested that drug–membrane interactions play a major role in the antioxidant capacity.^{5–8}

For all of the mentioned reasons, the study of the interaction between tolmetin and biomembranes is highly relevant and can contribute to the explanation of both the therapeutic and toxic effects of this NSAID. Although the therapeutic and toxic effects of tolmetin have been widely described, the biophysical mechanisms underlying these effects are far from being fully understood and seem to be closely connected with the interaction of this drug with lipid membranes.

Thereby, this work is focused on the application of different biophysical techniques to study the interaction of tolmetin with membrane mimetic models (liposomes, monolayers and supported lipid bilayers) composed of 1,2-dipalmitoyl-*sn*-glycero-3-phosphocholine (DPPC), used as a representative phospholipid of natural membranes.⁹ DPPC was also chosen for its suitability for modeling the interactions of NSAIDs and membranes, as it is

Received: June 26, 2011

Revised: September 19, 2011

Published: September 21, 2011

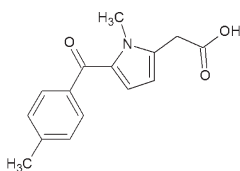


Figure 1. Chemical structure of tolmetin.

an endogenous component of the joints and represents approximately 45% of the total synovial fluid lipid component.¹⁰ Furthermore, DPPC is also adequate to understand the local deleterious effect of tolmetin on the GI tract, once the GI protective layer is composed predominantly of phosphatidylcholines (30–50%) with a large amount of the highly surface-active DPPC.¹¹ In this context, the membrane mimetic systems used constitute, both by their composition and different dimensionality, simple experimental systems that allow addressing the molecular interactions that can occur between tolmetin and biological membranes with reduced physical-chemical complexity when compared with natural membranes.

Besides the choice of appropriate membrane mimetic systems, care was taken to pursue the physiological conditions that tolmetin may find in the course of its *in vivo* therapeutic activity. Therefore, the studies performed covered the interactions of tolmetin with lipid membranes in both gel and liquid-crystalline phases. Liquid-crystalline or fluid phases are often evaluated in drug-membrane interaction studies. Although the fluid phase is the most biologically relevant, ordered domains are also present in biomembranes, and these domains share common properties with the lipid gel phase, a fact that is most times overlooked. Additionally, the interaction between tolmetin and lipid membranes in the gel phase is particularly interesting given that some inflammatory related enzymes, such as phospholipase A₂, require the presence of a lipid interface with both fluid and gel-like lipid domains to provide an adequate environment for lipid hydrolysis.^{12–14} Moreover, it is essential to study the interaction of tolmetin with lipid membranes in the gel phase once the gastric protective mucous layer is also a lipid membrane in the gel phase.¹⁵

In addition to the above-mentioned factors, the acid–base properties may also play a determinant role in the NSAIDs-membrane interactions, and this role has been scarcely studied. Indeed, the acid–base properties of tolmetin will motivate different ionization states according to the different biological environment found. Taking this in consideration, the biological pH values were further mimicked and all the studies were performed at two pH conditions: 7.4 simulating the plasma pH and 5 corresponding to the pH of inflamed tissues.

Not only the physiological conditions, but also the parameters evaluated, were a concern of the current work aiming to provide a complete picture of tolmetin-membrane interaction. In this regard, the different membrane mimetic models were associated with a wide range of biophysical techniques. Liposomes were used to determine: (i) the partition coefficient (K_p) of tolmetin between the lipid and the aqueous phases by derivative spectroscopy, (ii) the location of tolmetin within the membrane bilayer using steady-state fluorescence and lifetime quenching studies, and (iii) the influence of tolmetin on the thermotropic phase behavior of the membrane using fluorescence anisotropy.

The monolayers at the air/liquid interface allowed the study of the adsorption and penetration of tolmetin toward the membrane surface without interference of trans-bilayer events. In this

regard, isolated isotherm measurements and/or coupled with infrared reflection–absorption spectroscopy (IRRAS) were performed, allowing us to obtain structural information about the modifications in the membrane such as chain conformation, hydrogen bonding, and ionic bonds¹⁶ upon interaction of tolmetin with the phospholipids.

The interaction of tolmetin with the supported lipid bilayers (SLB) was assessed by atomic force microscopy (AFM), providing detailed morphological information on membrane phase separation.¹⁷

Therefore, the present study can be valuable to better understand the type of interaction between tolmetin and biomembranes, with the ultimate aim of relating these effects with some of the pharmacological and toxic properties of tolmetin.

MATERIALS AND METHODS

Materials. Tolmetin was obtained from Sigma-Aldrich, and DPPC was supplied by Avanti Polar-Lipids Inc. The fluorescence probe, trimethylammonium-diphenylhexatriene (TMA-DPH) was purchased from Molecular Probes (Invitrogen Corporation, Carlsbad, California, USA). All compounds were used without further purification. All other chemicals were purchased from Merck (Darmstadt, Germany).

Drug solutions were prepared either with Hepes buffer (pH 7.4) or Acetate buffer (pH 5) and the ionic strength ($I = 0.1 \text{ M}$) was adjusted with NaCl. The buffers were prepared using double-deionized water (conductivity inferior to $0.1 \mu\text{S cm}^{-1}$).

Preparation of Liposomes. Large unilamellar liposomes (LUVs with 100 nm diameter) of DPPC were prepared by the classical thin film hydration method, followed by extrusion through polycarbonate filters according to a previously described method.^{18–20} For the fluorescence techniques, TMA-DPH labeled liposomes were used. The probe was codried with the lipid in a ratio of 1:300 (probe:lipid).²¹

Determination of Partition Coefficients by Derivative Spectrophotometry. The partition coefficient (K_p) of tolmetin between LUVs suspensions of DPPC and aqueous buffered solution was determined by derivative spectrophotometry. Hepes buffered solution or Acetate buffered solution of tolmetin was added to liposomes containing a fixed concentration of drug ($40 \mu\text{M}$) and increasing concentrations of DPPC (100 – $1000 \mu\text{M}$). The correspondent reference solutions were identically prepared in the absence of drug. The absorption spectra of samples and references suspensions were recorded both in the gel phase ($30.0 \pm 0.1^\circ\text{C}$) and in the liquid-crystalline phase ($45 \pm 0.1^\circ\text{C}$) of DPPC, in a multidetection microplate reader (Synergy HT; Bio-Tek Instruments), accordingly to a well-established protocol,²² in the 220 – 520 nm range. The mathematical treatment of the results was performed using a developed routine, K_p Calculator,²² which (i) subtracts each reference spectrum from the correspondent sample spectrum to obtain corrected absorption spectra, (ii) determines the second and third derivative spectra in order to eliminate the spectral interferences due to light scattered by the lipid vesicles and to enhance the ability to detect minor spectral features and improve the resolution of bands, and (iii) calculates the K_p values in M^{-1} by a nonlinear fitting method.

Membrane Location Studies. The membrane location of tolmetin was assessed by steady-state fluorescence quenching and lifetime measurements using a fluorophore (TMA-DPH probe), with a well-established and documented membrane

position and depth.²³ The quenching studies were carried out by incubation of drugs with TMA-DPH labeled liposomes. A fixed concentration of DPPC was used ($500 \mu\text{M}$) and increasing concentrations of NSAIDs (0 – $100 \mu\text{M}$) buffered solutions were added to the labeled liposomes. Before fluorescence measurements, the resultant suspensions were incubated in the dark for 1 h at a temperature above the main phase transition temperature of DPPC (45°C), allowing tolmetin to reach the partition equilibrium between the lipid membranes and the aqueous medium. Measurements were carried out at four controlled temperatures in the range of 37 – 47°C for each pH value.

In steady-state fluorescence and lifetime quenching studies, excitation and emission wavelength were set to 361 and 427 nm , respectively.

Fluorescence steady-state measurements were performed in a Perkin-Elmer LS-50 B spectrophotometer equipped with a constant temperature cell holder. All data were recorded in a 1 cm path length cuvette. For each measurement, fluorescence emission was automatically acquired during 30 s . Fluorescence intensity values were corrected for inner filter effects at the excitation wavelength.²⁴

Fluorescence lifetime measurements were made with a Fluorolog Tau-3 Lifetime system. Modulation frequencies were acquired between 6 and 200 MHz . Integration time was 10 s . Manual slits were 0.5 mm , slits for excitation monochromator were 7.0 (side entrance) and 0.7 mm (side exit) and for emission monochromator 7.0 (side entrance) and 7.0 mm (side exit). The fluorescence emission was detected with a 90° scattering geometry. All measurements were made using Ludox as a reference standard ($\tau = 0.00 \text{ ns}$).

Phase Transition Temperature Studies. To complement the information provided by quenching data, fluorescence anisotropy with the TMA-DPH probe was used to study the effect of tolmetin on the membrane main transition temperature (T_m) and thus infer about the influence of this compound on membrane fluidity. A fixed concentration of tolmetin ($40 \mu\text{M}$) in the DPPC suspension ($500 \mu\text{M}$) was used at both pH conditions. The transition temperature was assessed by fluorescence anisotropy measurements in a Perkin-Elmer LS 50B steady-state fluorescence spectrometer equipped with a constant-temperature cell holder. All data were recorded in 1 cm cuvettes with excitation and emission slits between 2.8 and 3.0 nm . The excitation and emission wavelengths were set to 361 and 427 nm , respectively. The anisotropy was recorded at several temperatures between 28.0 and 52.0°C , with an accuracy of 0.1°C .

Langmuir Isotherms and Infrared Reflection Absorption Spectroscopy Measurements. Surface pressure–area isotherms (π/A) were performed in a PTFE Langmuir trough (Riegler & Kirstein, Potsdam, Germany), equipped with barriers for changing the surface area, and a Wilhelmy microbalance with filter paper plate (accuracy superior to 0.1 mN m^{-1}) for measuring the surface pressure of the monolayer.

Monolayers of DPPC were obtained after spreading phospholipid/chloroform solutions (1 mM) on the buffer subphase (Hepes or Acetate buffer) or on solutions containing tolmetin ($50 \mu\text{M}$) prepared with the same buffers.

After an equilibration time of 10 min , the monolayers were compressed at a rate of $5 \text{ \AA}^2/\text{molecule/min}$. Before each measurement, the trough was cleaned thoroughly with chloroform and double-deionized water. Cleanliness was confirmed by compressing a water subphase and achieving a zero surface pressure reading. All measurements were performed at 23°C .

For the infrared reflection absorption spectroscopy measurements (IRRAS) an IFS 66 FT-IR spectrometer from Bruker (Ettlingen, Germany) equipped with an external reflectance unit containing a Langmuir trough setup (R & K) and a liquid nitrogen-cooled MCT detector was used. The IR beam is directed through the external port of the spectrometer and is subsequently reflected by three mirrors in a rigid mount before being focused on the water surface of the Langmuir trough. The angle of incidence of the IR beam, polarized by a KRS-5 (thallium bromide and iodide mixed crystal) wire grid polarizer perpendicular to the plane of incidence (s), with respect to the surface normal was 40° . The reflected light was collected at the same angle as the angle of incidence. Measurements were made by switching between two interconnected troughs (to ensure the same surface height on both sides) at regular intervals using a trough shuttle system controlled by the acquisition computer. One trough contained the monolayer system under investigation (sample), whereas the other (reference) is filled with the pure subphase. The spectra from the reference trough were subtracted from the sample spectra in order to eliminate the water vapor signal. To reduce relative humidity fluctuations, the setup was placed in a hermetically sealed container. Spectra were recorded with a spectral resolution of 8 cm^{-1} and accumulated using 400 scans.

Atomic Force Microscopy (AFM) Measurements. The AFM studies were performed in supported lipid bilayers (SLB). The SLB were prepared by the fusion of LUVs onto solid supports of freshly cleaved mica according to a previously reported procedure²⁵ using the two different buffers with pH values of 5.0 and 7.4 (Acetate and Hepes buffers, respectively).

AFM images were taken using a Nanoscope III AFM in tapping mode (Veeco/Digital Instruments, Santa Barbara, CA). Cantilevers with 0.01 N m^{-1} spring constants and oxide-sharpened tips in the liquid cell (multimode liquid cell using O-ring) were used. At least three regions of the surface were examined to verify if similar morphology existed throughout the sample. After recording the lipid bilayer in buffer and choosing an image of a region of interest, that is, a region which is representative of the entire SLB, the O-ring pump adapted with syringe was used to exchange the buffer with the tometin solution (1 mM). Several images were recorded for at least 2 h . The images were analyzed using the Nanoscope V software from the AFM supplier.

■ RESULTS AND DISCUSSION

Determination of Tolmetin Partition Coefficients by Derivative Spectroscopy. Lipophilicity is a physicochemical property that extensively influences the pharmacokinetic and pharmacodynamic profile of drugs. In this context, the determination of the partition coefficient (K_p), which provides an indication of the distribution of drugs between aqueous and lipid phases, is of great interest once it facilitates the prediction and understanding of the passive diffusion processes across biological barriers that conditions the drugs' absorption, distribution, metabolism, and elimination processes and can be correlated with their toxic and/or therapeutic effects.²⁶

Traditionally, the partition coefficients are determined in octanol/water systems. However, liposome/water systems provide an anisotropic environment similar to the one of the natural membranes and allow establishing electrostatic interactions between drugs and the polar groups of the phospholipids which cannot be assessed in a biphasic octanol/water system.^{5,26} Furthermore, derivative spectroscopic techniques combined

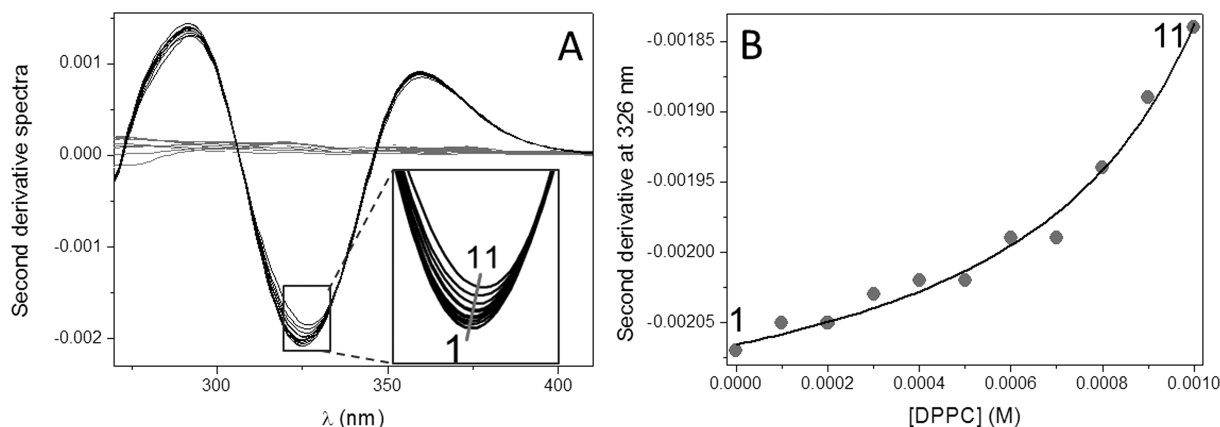


Figure 2. Second-derivative spectra (A) of tolmetin at pH 7.4 ($40\text{ }\mu\text{M}$) incubated in LUVs of DPPC in Hepes buffer at $30\text{ }^\circ\text{C}$ (black lines) and LUVs of DPPC without drug (gray lines) at different lipid concentrations (M), from 1 to 11 which represents the increasing concentrations of DPPC. Panel B represents the fitting curve to experimental second-derivative spectrophotometric data as a function of DPPC concentration, using a nonlinear least-squares regression method at wavelength 326 nm where the scattering is eliminated.

with liposome/water systems allow determining the drug distribution between the lipid and aqueous media, without the necessity to quantify the drug separately in each media.²⁷ Moreover, the background signals of liposome light scattering can be easily eliminated by the use of derivative spectrophotometry that additionally provides a better resolution of overlapped bands.^{22,27}

In Figure 2A is presented, as an example, the second derivative of the absorbance spectra of tolmetin with different concentrations of LUVs of DPPC at pH 7.4 and at $30\text{ }^\circ\text{C}$. The isosbestic points observed in Figure 2A indicate that the influences of the residual background signal of LUVs are entirely eliminated in the second derivative of the spectra.^{22,28,29} Furthermore, the derivative spectra of tolmetin in LUVs of DPPC exhibits a shift of 5 nm in the λ_{\min} with increasing lipid concentration (see the inset detail in Figure 2A), an observation that provides a clear indication that the drug partitions from the aqueous to the lipid media.²²

K_p values were obtained by a nonlinear least-squares regression method³⁰ at wavelengths where the scattering is eliminated, in the case of tolmetin 326 nm (Figure 2B).

The liposomes aqueous partition coefficients of tolmetin were determined at two different temperatures at which DPPC is in the gel phase ($30.0 \pm 0.1\text{ }^\circ\text{C}$) and in the liquid-crystalline phase ($45.0 \pm 0.1\text{ }^\circ\text{C}$) and at pH 7.4 and 5. The values of K_p obtained are listed in Table 1.

When focusing on the liquid-crystalline phase of DPPC, analysis of the values presented in Table 1 reveals that tolmetin exhibits a similar membrane partitioning at both pH conditions. Tolmetin has a pK_a value of 3.5,³¹ and calculations of the degree of ionization (using Marvin software from Chemaxon) reveal that, at pH 7.4, 99.9% of tolmetin molecules are in the anionic form (correspondent to the deprotonation of the carboxyl group), and this form also predominates (92.0%) at pH 5.0. However, a neutral form of tolmetin is also found (8.0%) at this latter pH. The similar ionization degree of the drug explains the comparable K_p values obtained for both pH conditions, suggesting that the negatively charged tolmetin interacts with the phospholipid polar head groups, possibly by establishing electrostatic interactions with the positively charged choline. In the gel phase of DPPC, the membrane partitioning of tolmetin was more pronounced for pH 5 than for pH 7.4, what is consistent with the existence of a neutral state of the drug at the former pH that is

Table 1. Partition Coefficients of Tolmetin in LUVs of DPPC at pH 5.0 and 7.4, at the Gel and Fluid Phases

pH	DPPC phase	temperature ($^\circ\text{C}$)	$K_p (\text{M}^{-1})$
5.0	gel	30	846 ± 7
	liquid-crystalline	45	804 ± 41
7.4	gel	30	732 ± 38
	liquid-crystalline	45	819 ± 42

able to have a deeper access into the hydrophobic core of the membrane.

The K_p values obtained were also used to assess the membrane effective concentrations of tolmetin ($[Q]_m$), by the following equation:^{32,33}

$$[Q]_m = \frac{K_p [Q]_T}{K_p \alpha_m + (1 - \alpha_m)}$$

where α_m is the volume fraction of membrane phase ($\alpha_m = V_m/V_T$; V_m and V_T represent the volumes of the membrane and water phases, respectively) and $[Q]_T$ is the total concentration of tolmetin. The calculation of the membrane effective concentrations was required for the subsequent fluorescent quenching studies of membrane location, because only the drug molecules that are distributed in the membrane will be able to quench the fluorophore inserted in the lipid bilayers. Therefore membrane effective concentrations of tolmetin ($[Q]_m$) will be used instead of the total concentration of drug ($[Q]_T$).

Drug Location Studies. The location of a drug in the membrane can be tracked by fluorescence quenching of a membrane bound probe (with a well-defined location in the membrane), once this technique provides a measure of the accessibility of the drug to the probe.³³ According to this, in the current study the steady-state fluorescence intensities and lifetimes were measured in liposomes labeled with TMA-DPH probe. The quenching of fluorescence was analyzed by the modified Stern–Volmer equation⁵

$$\frac{I_0}{I} = K_{SV}[Q]_m + 1$$

where I and I_0 are the fluorescence steady state intensities with and without the quencher (tolmetin), respectively, K_{SV} is the

Table 2. Values of the Stern–Volmer Constant (K_{SV}) Obtained for Tolmetin in LUVs of DPPC Labeled with TMA-DPH at pH 5.0 and 7.4 at Different Temperatures

pH	temperature (°C)	$K_{SV} (M^{-1})$
5.0	37	14.06 ± 0.02
	40	13.87 ± 0.05
	42	13.56 ± 0.03
	45	12.07 ± 0.02
7.4	37	14.69 ± 0.01
	42	13.99 ± 0.02
	45	12.514 ± 0.06
	47	11.14 ± 0.06

Stern–Volmer constant and $([Q]_m)$ is the membrane effective concentration of tolmetin.

The molecular contact between the probe (fluorophore) and the drug (quencher) can be due to diffusive encounters, which is dynamic quenching, or due to complex formation, which is static quenching.³³ Static and dynamic quenching can be distinguished by their different dependence on temperature, and additionally by lifetime measurements.³³ Therefore, in order to access the type of quenching between tolmetin and the TMA-DPH probe, fluorescence quenching studies (steady-state and lifetime) were performed at different temperatures for each pH value. In the case of static quenching, higher temperatures will result in the dissociation of weakly bound complexes,³³ and hence, lower values of K_{SV} will be obtained. In fact, results show that at both pH conditions, the K_{SV} value decreases with temperature (Table 2). This, along with the fact that $\tau_0/\tau \approx 1$ (Figure 3), leads to the conclusion that the quenching of tolmetin with TMA-DPH is of static nature.

TMA-DPH is reported as being anchored in the polar head groups region of phospholipids due to its charged group and hence is located closer to the lipid/water interface.³⁴ Accordingly, as the quenching mainly occurs by the formation of a nonfluorescent ground-state complex between the probe and tolmetin (static quenching), this suggests, once again, that tolmetin may be bound electrostatically to the head groups of phospholipids and hence concentrated on the surface of the liposomes. Similar behavior has been observed with other ionic compounds that are electrostatically bound to the headgroup of phospholipid vesicles and thus located within an interaction radius of the system fluorophore-quenching, acting as static quencher of fluorophores with similar locations.^{35,36}

Phase Transition Temperature Studies. The evaluation of the phase transition temperature was based on the change of fluidity of the DPPC liposomes from the gel phase to the liquid-crystalline phase, which was assessed by fluorescence anisotropy. Small changes in the stiffness of the matrix surrounding the fluorescent probe (in this case TMA-DPH) induce changes on its rotational movement and thereby promote changes in anisotropy. The temperature dependence of TMA-DPH fluorescence anisotropy in DPPC liposomes in the presence and absence of tolmetin is shown in Figure 4.

From the experimental data displayed it was possible to calculate the cooperativity (B) and the midpoint of the phase transition, which corresponds to the main phase transition temperature of DPPC (T_m), calculated from the slope and the inflection point of the data fitted to sigmoid curves of steady-state anisotropy versus temperature (°C).³⁷

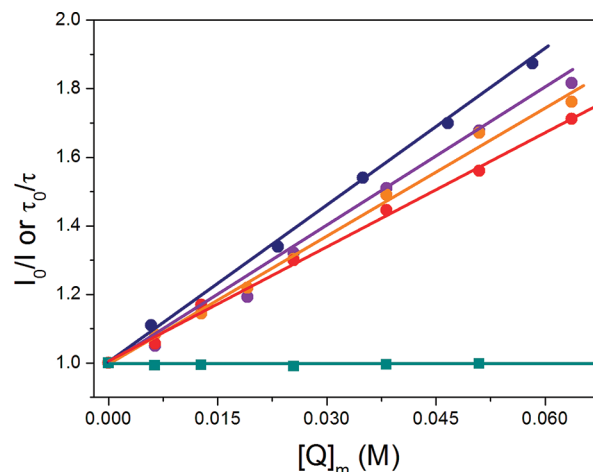


Figure 3. Stern–Volmer plots of the probe TMA-DPH in LUVs of DPPC at pH 7.4 by increasing concentrations (M) of tolmetin at 37 °C (dark blue circle), 40 °C (purple circle), 45 °C (orange circle), and 47 °C (red circle). Circles represent Stern–Volmer plot obtained by steady-state fluorescence measurements (I_0/I) and squares represent Stern–Volmer plot obtained by lifetime fluorescence measurements (τ_0/τ).

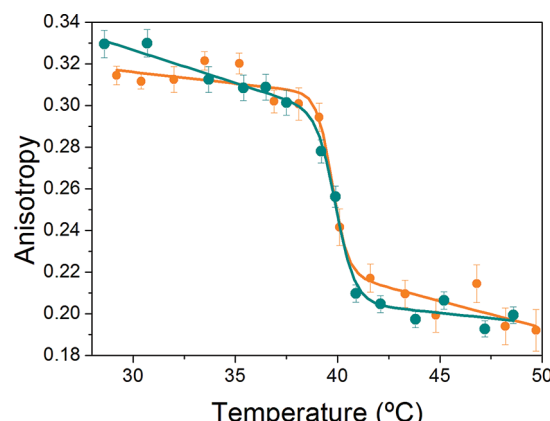


Figure 4. Steady-state anisotropy of TMA-DPH in absence (blue-green circle) and in the presence (orange circle) of tolmetin in DPPC liposomes (pH 5.0) as a function of temperature. Continuous lines are the best fitted curves.

Table 3. Values of Cooperativity (B) and Main Phase Transition Temperature (T_m), Obtained for DPPC Liposomes Labeled with TMA-DPH at pH 5.0 and 7.4 in the Absence and in the Presence of Tolmetin

	pH	cooperativity (B)	T_m (°C)	R^2
DPPC	5.0	1502 ± 240	39.93 ± 0.08	0.990
DPPC + tolmetin		1854 ± 700	39.7 ± 0.2	0.992
DPPC	7.4	898 ± 43	42.21 ± 0.05	0.998
DPPC + tolmetin		683 ± 94	38.9 ± 0.1	0.991

For all the studied systems, the values of cooperativity (B) and main phase transition temperature (T_m) are presented in Table 3.

At pH 7.4 the incorporation of tolmetin lowered the T_m of pure DPPC by approximately 3 °C and also affected significantly the cooperativity (B) of the transition. These findings are in

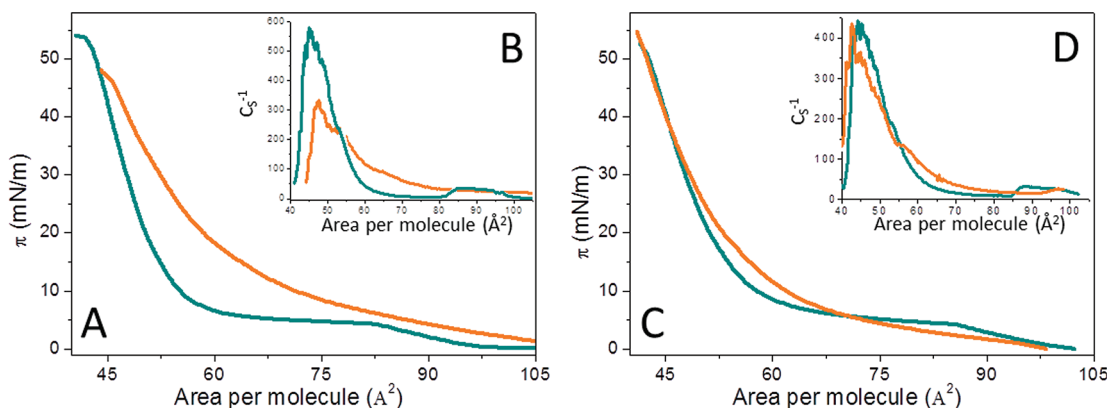


Figure 5. Surface pressure/area (π/A) isotherms of DPPC in buffer (blue-green line) and in tolmetin subphase (orange line), at pH 5.0 (A) and pH 7.4 (C). Insets B and D represent the correspondent elastic modulus for the isotherms represented in panels A and C.

agreement with an electrostatic interaction between the drugs and the headgroup of the phospholipids³⁷ previously reported.

At pH 5 and at temperatures below T_m , tolmetin induces a decrease in the r_s values (Figure 4). Since it was observed that addition of tolmetin did not promote relevant alterations of the fluorescence lifetime of the probe TMA-DPH (Figure 3), the decrease of anisotropy is therefore consistent with an increase of the rotational motion of the probe indicating that tolmetin is able to fluidize the membrane in the gel phase. These results provide evidence for the interaction of tolmetin with the lipid bilayers even in the more ordered phase, which is in agreement with the above-mentioned partition coefficient studies.

Langmuir Isotherms and Infrared Reflection Absorption Spectroscopy Measurements. In studies of interactions of molecules with lipid monolayers there are two important parameters that should be focused: the location of the guest molecule in the monolayer, and the changes in film fluidity and permeability due to the incorporation of such molecules.³⁸ Moreover, the calculation of the elastic modulus (C_s^{-1})³⁹ is also useful to assess the elastic properties of the Langmuir monolayers. In general, a higher value of C_s^{-1} indicates a less compressible membrane.

Figure 5 shows that the surface pressure-area (π/A) isotherm of a DPPC monolayer was affected to different extents by the presence of tolmetin depending on the pH. Moreover, the π/A isotherm of DPPC at pH 7.4 and at pH 5 are in good agreement with the literature.^{40,41}

At pH 5, the presence of tolmetin causes a clear decrease in C_s^{-1} of the condensed part of the DPPC monolayer indicating a better compressible monolayer. The whole isotherm is shifted to larger areas what can be explained by a penetration of tolmetin into the DPPC monolayer. The phase transition cannot be clearly identified since compression of the layer leads to a partial squeezing out of the drug. However, the area per lipid molecule is still larger on the tolmetin subphase even at high pressures. The extrapolated minimal area at zero pressure (A_{\min}) is remarkably increased from 53.8 to 61.0 $\text{\AA}^2/\text{molecule}$. This shows that the drug is not completely expelled from the monolayer upon compression up to the collapse pressure.

At pH 7.4, the presence of tolmetin causes a much smaller increase in A_{\min} from 53.4 to 54.9 $\text{\AA}^2/\text{molecule}$. This shows that much less tolmetin has penetrated into the condensed lipid monolayer, what might be consistent with the fact of tolmetin being exclusively negatively charged at this pH and, as such,

interacting mainly electrostatically with the polar phospholipid head groups. Even at low pressure, the isotherm is not shifted to larger molecular areas. Only the phase transition is not as cooperative as on the pure buffer. A similar effect was also reported for other NSAIDs (ibuprofen and diclofenac) that cause a destabilization of the phospholipid intermolecular cooperativity.⁴² The larger effect is observed in the condensed phase at pressures between 5 and 30 mN/m. The observed shift to larger areas could be an indication of a partial penetration or of a change in the DPPC monolayer structure (larger tilt induced by interactions of tolmetin with the head groups). On compression, this effect is progressively diminished, and at higher lateral pressures the isotherms of DPPC in the absence or presence of tolmetin are almost superimposed.

In order to complete the information of the Langmuir isotherms in terms of chain conformation, hydrogen bonding and ionic interactions, infrared reflection-absorption spectroscopy (IRRAS) measurements were performed.

Measurements have been performed at two different pressures (LE/LC transition region at $\pi = 5 \text{ mN/m}$ and LC phase at $\pi = 30 \text{ mN/m}$) on both pH subphases. Selected band positions are presented in Table 4.

The symmetric and asymmetric wavenumbers of the methylene stretching vibrations [$\nu_s(\text{CH}_2)$ and $\nu_{as}(\text{CH}_2)$], around 2850 and 2920 cm^{-1} respectively are used to characterize the state of conformational order in the lipid monolayer.^{16,43} The wavenumber values can be used to monitor the average trans/gauche isomerization in the systems. Accordingly, as the pressure increases (from $\pi = 5$ –30 mN/m), the $\nu_s(\text{CH}_2)$ and $\nu_{as}(\text{CH}_2)$ bands of the pure DPPC monolayers (at both pH conditions) are shifted to lower wavenumbers (Table 4) which indicates an increase in the number of trans conformers, i.e., an increase of the acyl chains conformational order.¹⁶ Furthermore, at pH 5 and for both surface pressures assayed ($\pi = 5$ and 30 mN/m), the $\nu_s(\text{CH}_2)$ and $\nu_{as}(\text{CH}_2)$ bands appear at lower wavenumbers than at pH 7.4 (Table 4), suggesting that the monolayer is more ordered at lower pH values. This is in good agreement with the compression isotherm studies where a higher value of C_s^{-1} was observed at pH 5 indicating a less compressible layer at this pH.

Regarding the effect of tolmetin, it is possible to conclude that this NSAID interacts with different phospholipid groups according to the pH of study. From the previous analysis of the Langmuir isotherms, it seemed that, because being exclusively negatively charged at pH 7.4, tolmetin would interact

Table 4. Wavenumbers of Different Vibrations in DPPC Monolayers on the Aqueous Subphases Containing Tolmetin at pH 5.0 and 7.4 for $\pi = 5$ and 30 mN/m

subphase	$\pi = 5$ mN/m				$\pi = 30$ mN/m			
	$\nu_s(\text{CH}_2)$ (cm ⁻¹)	$\nu_{\text{as}}(\text{CH}_2)$ (cm ⁻¹)	$\nu_{\text{as}}(\text{PO}^{2-})$ (cm ⁻¹)	$\nu(\text{CO})$ (cm ⁻¹)	$\nu_s(\text{CH}_2)$ (cm ⁻¹)	$\nu_{\text{as}}(\text{CH}_2)$ (cm ⁻¹)	$\nu_{\text{as}}(\text{PO}^{2-})$ (cm ⁻¹)	$\nu(\text{CO})$ (cm ⁻¹)
acetate	2851	2920	1228	1732	2850	2918	1227	1738
tolmetin	2854	2924	1222	1731	2851	2920	1230	1739
hepes	2852	2920	1246	1739	2851	2919	1242	1739
tolmetin	2851	2920	1227	1737	2852	2921	1227	1737

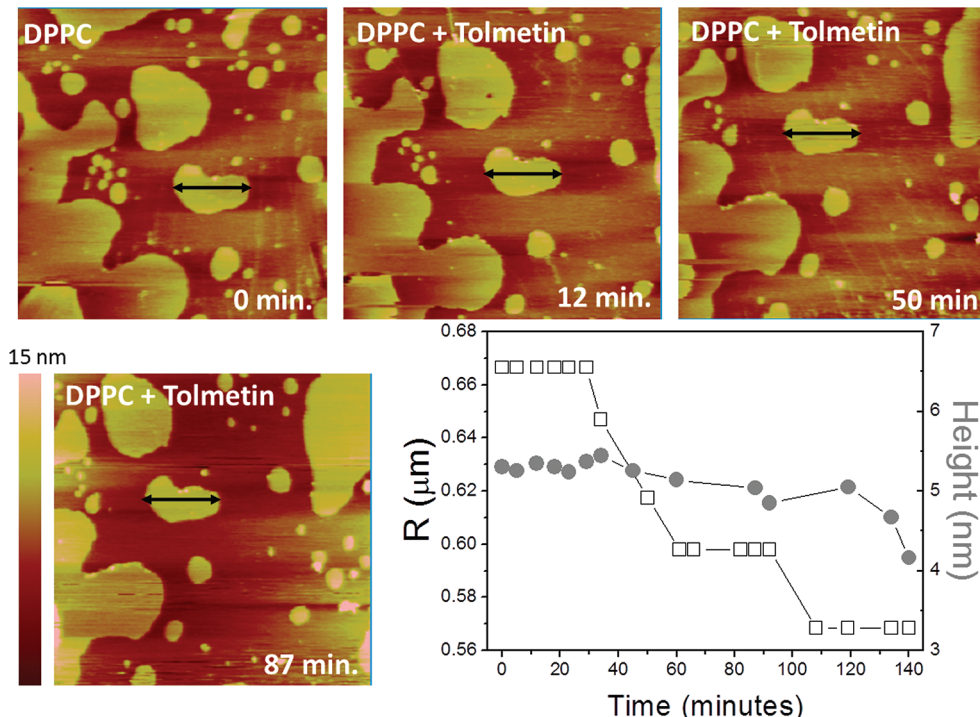


Figure 6. AFM images of DPPC supported lipid bilayer at pH 7.4 in the presence of tolmetin with different incubation times and graphical representation of the radius (open squares) and height (solid circles) of the signed patch.

preferentially with the headgroup region of the monolayers. This preferential interaction is confirmed by the shift of the $\nu_{\text{as}}(\text{PO}^{2-})$ to much smaller values compared with pure DPPC (Table 4) (for both pressures), indicating the establishment of more hydrogen bonds¹⁶ between the polar head groups and tolmetin. In addition, at the same pH, the $\nu_s(\text{CH}_2)$ and $\nu_{\text{as}}(\text{CH}_2)$ are almost unchanged by the presence of tolmetin (Table 4) and the effect of $\nu(\text{C=O})$ vibration is negligible which also confirms the interaction of tolmetin with head groups, without penetration into the hydrophobic core of the monolayer. Similar observations were made for other NSAIDs (e.g., ibuprofen and diclofenac that share the same chemical carboxyl moiety in the anionic form at pH 7.4) for which FTIR-ATR studies revealed that the drugs are located preferentially in the polar head groups of the phospholipids.⁴²

At pH 5, there are indications that tolmetin is not only able to establish electrostatic interactions with the polar head groups, but is also able to penetrate into the hydrophobic core of the lipid monolayer. Indeed, although at $\pi = 5$ mN/m a small shift of the $\nu_{\text{as}}(\text{PO}^{2-})$ can be observed, indicative of hydrogen bonding of

tolmetin to the phospholipids' head groups, the shift of the $\nu_s(\text{CH}_2)$ and $\nu_{\text{as}}(\text{CH}_2)$ vibrations to lower wavenumbers also occurs and remains at higher pressures ($\pi = 30$ mN/m) indicating an interaction of tolmetin with the hydrophobic chains of the monolayer (Table 4). These findings confirm the previous Langmuir isotherms, where an enhanced penetration of the drug into the lipid monolayer was observed at pH 5.

Atomic Force Microscopy (AFM) Measurements. Atomic force microscopy (AFM) has shown to be ideally suited to obtain detailed morphological information on phase separation in supported lipid monolayers and bilayers,¹⁷ making also possible to follow the evolution of the interaction of drugs, peptides or other molecules.⁴⁴

Upon exposing LUVs suspension to a mica surface, vesicles adhere to the surface, suffering rupture, and forming a planar supported lipid bilayer (SLB).²³

In this work, the measured height of the SLB was in average 5.0 nm which is the typical value for a DPPC bilayer.⁴⁵ After the injection of tolmetin, time-lapsed AFM images were recorded at both pH conditions and at the same location as the SLB before

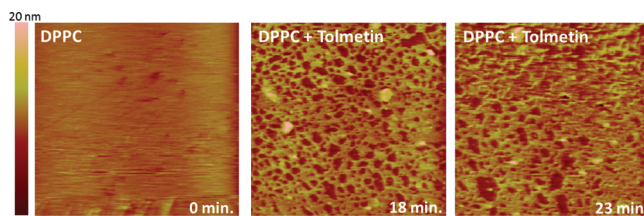


Figure 7. AFM images of DPPC supported lipid bilayer at pH 5.0 in the presence of tolmetin with different incubation times.

injection of the drug. At pH 7.4, a progressive decrease of the size of DPPC patches of SLB in the gel phase can be seen with time (Figure 6). The patches gradually shrink in size and height.

From this observation it is possible to conclude that tolmetin interacts with the SLB at pH 7.4 promoting a progressive disruption of small DPPC gel patches. On the basis of what has been reported about the main gel-to-liquid crystalline phase transition, the observed height decrease of ~ 1 nm after interaction of tolmetin with SLB of DPPC can be attributed to a fluidizing effect of the drug.⁴⁶

At pH 5.0, the effect of tolmetin is also evident as a time-dependent erosion of DPPC gel domains. The consequence of drug interaction with SLB is a decrease of the surface covered by the bilayer with the appearance of several holes in the bilayer (Figure 7). Furthermore, the size and number of holes increase with the time of interaction between the SLB and the drug.

CONCLUSIONS

The complete mechanisms underlying the GI toxicity of NSAIDs are unknown, but the nonselectivity to COX-2 and the local effect of drugs at the GI protective mucosa have been implicated in the serious adverse GI events. Although several studies have been conducted to evaluate the role of COX selectivity in GI toxicity of NSAIDs, less attention has been paid on the biophysical effects of the interaction of NSAIDs with membranes. Tolmetin is a NSAID very effective in the treatment of inflammation and in the relieve of pain, however the adverse effects on the gastrointestinal tract, including induction of ulcers and hemorrhage have hindered the use of this drug, nowadays restricted to postchirurgical applications.

The facility of tolmetin to interact and penetrate the lipid bilayer of biomembranes, causing variations in their structure and fluidity, may be one of the major causes influencing secondary effects exerted by this compound on gastric mucosa. Indeed, zwitterionic phospholipids line the luminal aspects of the GI gel layer conferring protection against the acid damage and the ability to interact with zwitterionic phospholipids is pointed out as a possible mechanism by which NSAIDs compromise the integrity of protective lipid barrier. Therefore, the current study provided more insight into the molecular mechanism by which tolmetin acts at the membrane level, and demonstrated using several techniques, the effect of this NSAID on the biophysical properties of membrane systems (liposomes, monolayers and SLBs) used as models for cellular membranes and for the GI gel protective layer.

Tolmetin revealed a deep interaction with the membrane mimetic models and the effects of this NSAID on the membranes was essentially dependent on the pH of the medium and on the lipid phase studied. At pH 7.4, tolmetin is negatively charged, and thus, the drug interactions with the lipid polar head groups are predominant. At pH 5, the anionic form of tolmetin still predominates, but the

neutral counterpart is also apparent. Therefore the nature of the drug—membrane interactions at pH 5 is also hydrophobic.

Hence, the ionization of tolmetin has important implications in the interaction of this drug with the membrane. Accordingly, the negatively charged carboxyl group is able to establish electrostatic interactions with the positively charged choline from the phospholipid polar head groups, and this fact is consistent with the quenching studies that pointed to a location of tolmetin at the membrane surface. The results obtained from the studies in monolayers also reflect the effect of the different ionic forms of tolmetin on the interaction of this drug with the membrane. Indeed, at pH 7.4, an increase of the hydrogen bonds to the polar phosphate groups was observed consistent with a preferential interaction of tolmetin with the headgroup region of the lipid monolayers. On the other hand, at pH 5, an increase in the molecular area observed in surface pressure-area isotherms indicated that tolmetin penetrates into the lipid monolayer and establishes hydrophobic interactions with the phospholipid acyl chains. This was further confirmed by IRRAS measurements where it was observed that, at pH 5, tolmetin interacts with the CH₂ groups of the acyl chains.

The overall results obtained at both pH values indicate that tolmetin locates at the membrane surface and establishes a strong interaction with the membrane independently of the drug being exclusively located at the headgroup region or presenting some penetration at the hydrophobic core. These results can explain the great therapeutic efficacy of tolmetin, due to the drug accumulation in membranes that lead to much larger concentrations at the active site than in the surrounding aqueous phase.

Besides considering the pH, it is also important to take the lipid phase state into account. The gel phase and the more acidic pH are the most relevant parameters to establish a correlation between the biophysical effects of tolmetin and its local toxic effects at the gastric mucosa. Accordingly the membrane disturbance induced by tolmetin was more pronounced for the gel phase at pH 5, what is consistent with the expected effect of this drug at the GI level. Indeed, in the gel phase and at pH 5, tolmetin demonstrated higher membrane partitioning, probably due the existence of a neutral form of the drug that is able to have a deeper access into the hydrophobic core of the membrane in the more ordered phase. Anisotropy studies corroborate the disturbing effects of tolmetin in the lipid gel phase at acidic conditions that include a decrease in the lipid microviscosity. This aspect is consistent with the time-dependent erosion of SLB gel domains observed by AFM that can be interpreted as a membrane fluidizing effect of the drug.

AUTHOR INFORMATION

Corresponding Author

*Tel: +351-222078966. Fax: +351-222078961.

ACKNOWLEDGMENT

C.N. thanks FCT for the doctoral grant (SFRH/BD/38445/2007). We also thankfully acknowledge Anneliese Heilig and Ana Saraiva (MPI-KG, Potsdam, Germany) for helping with AFM measurements.

REFERENCES

- Olsen, J.; Li, C. Z.; Skonberg, C.; Bjornsdottir, I.; Sidenius, U.; Benet, L. Z.; Hansen, S. H. *Drug Metab. Dispos.* 2007, 35, 758–764.

- (2) Parfitt, K. *The complete drug reference*, 32nd ed.; Pharmaceutical Press: London, 1999.
- (3) Escriba, P. V. *Trends Mol. Med.* **2006**, *12*, 34–43.
- (4) Fernandes, E.; Costa, D.; Toste, S. A.; Lima, J. L. F. C.; Reis, S. *Free Radical Biol. Med.* **2004**, *37*, 1895–1905.
- (5) Lucio, M.; Nunes, C.; Gaspar, D.; Golebska, K.; Wisniewski, M.; Lima, J. L. F. C.; Brezesinski, G.; Reis, S. *Chem. Phys. Lett.* **2009**, *471*, 300–309.
- (6) Lucio, M.; Nunes, C.; Gaspar, D.; Ferreira, H.; Lima, J. L. F. C.; Reis, S. *Food Biophys.* **2009**, *4*, 312–320.
- (7) Lucio, M.; Ferreira, H.; Lima, J. L.; Reis, S. *Anal. Chim. Acta* **2007**, *597*, 163–170.
- (8) Reis, S.; Lucio, M.; Segundo, M. A.; Lima, J. L. F. C. Use of Liposomes to Evaluate the Role of Membrane Interactions on Antioxidant Activity. In *Liposomes Methods and Protocols*; Weissig, V., Ed.; Humana Press: New York, 2010; Vol. 2: Biological Membrane Models; pp 167–188.
- (9) Gambinossi, F.; Puggelli, M.; Gabrielli, G. *Colloids Surf. B-Biointerfaces* **2002**, *23*, 273–281.
- (10) Jordan, O.; Butoescu, N.; Doelker, E. *Eur. J. Pharm. Biopharm.* **2009**, *73*, 205–218.
- (11) Mosnier, P.; Rayssiguier, Y.; Motta, C.; Pelissier, E.; Bommelaer, G. *Gastroenterology* **1993**, *104*, 179–184.
- (12) Seddon, A. M.; Casey, D.; Law, R. V.; Gee, A.; Templer, R. H.; Ces, O. *Chem. Soc. Rev.* **2009**, *38*, 2509–2519.
- (13) Gaspar, D.; Lucio, M.; Wagner, K.; Brezesinski, G.; Rocha, S.; Lima, J. L. F. C.; Reis, S. *Biophys. Chem.* **2010**, *152*, 109–117.
- (14) Dahmen-Levison, U.; Brezesinski, G.; Mohwald, H.; Jakob, J.; Nuhn, P. *Angew. Chem., Int. Ed. Engl.* **2000**, *39*, 2775–2778.
- (15) Allen, A.; Flemstrom, G. *Am. J. Physiol.-Cell Physiol.* **2005**, *288*, C1–C19.
- (16) Mendelsohn, R.; Flach, C. R. *Peptide-Lipid Interact.* **2002**, *52*, 57–88.
- (17) Yuan, C. B.; Johnston, L. J. *Biophys. J.* **2001**, *81*, 1059–1069.
- (18) Lasic, D. D. *Liposomes - from Physics to Applications*; Elsevier: New York, 1993.
- (19) Lucio, M.; Ferreira, H.; Lima, J. L. F. C.; Matos, C.; de Castro, B.; Reis, S. *Phys. Chem. Chem. Phys.* **2004**, *6*, 1493–1498.
- (20) Brittes, J.; Lucio, M.; Nunes, C.; Lima, J. L. F. C.; Reis, S. *Chem. Phys. Lipids* **2010**, *163*, 747–754.
- (21) New, R. R. C. *Liposomes - a practical approach*; Oxford University Press: New York, 1990.
- (22) Magalhaes, L. M.; Nunes, C.; Lucio, M.; Segundo, M. A.; Reis, S.; Lima, J. L. F. C. *Nat. Protocols* **2010**, *5*, 1823–1830.
- (23) Repáková, J.; Capková, P.; Holopainen, J. M.; Vattulainen, I. *J. Phys. Chem. B* **2004**, *108*, 13438–13448.
- (24) Coutinho, A.; Prieto, M. *J. Chem. Educ.* **1993**, *70*, 425.
- (25) Mingeot-Leclercq, M. P.; Deleu, M.; Brasseur, R.; Dufrene, Y. F. *Nat. Protocols* **2008**, *3*, 1654–1659.
- (26) Seydel, J. K.; Wiese, M. Drug-Membrane Interactions: Analysis, Drug Distribution, Modeling. In *Methods and Principles in Medicinal Chemistry*; Mannhold, R., Kubinyi, H., Folkers, G., Eds.; Wiley-VCH: Weinheim, Germany, 2002; Vol. 15, pp 35–49.
- (27) Ferreira, H.; Lúcio, M.; Castro, B.; Gameiro, P.; Lima, J. L. F. C.; Reis, S. *Anal. Bioanal. Chem.* **2003**, *377*, 293–298.
- (28) Takegami, S.; Kitamura, K.; Kitade, T.; Hasegawa, K.; Nishihira, A. *J. Colloid Interface Sci.* **1999**, *220*, 81–87.
- (29) Hendrich, A. B.; Wesolowska, O.; Pola, A.; Motohashi, N.; Molnar, J.; Michalak, K. *Mol. Membr. Biol.* **2003**, *20*, 53–60.
- (30) Magalhaes, L. M.; Segundo, M. A.; Reis, S.; Lima, J. L. *Anal. Chim. Acta* **2008**, *613*, 1–19.
- (31) Cantabrana, B.; Vallina, J. R. P.; Menendez, L.; Hidalgo, A. *Life Sci.* **1995**, *57*, 1333–1341.
- (32) Lúcio, M.; Ferreira, H.; Lima, J. L. F. C.; Reis, S. *Med. Chem.* **2006**, *2*, 447–456.
- (33) Lakowicz, J. R. *Principles of Fluorescence Spectroscopy*, 3rd ed.; Springer: New York, 2006.
- (34) Illinger, D.; Duportail, G.; Mely, Y.; Poirelmoires, N.; Gerard, D.; Kuhry, J. G. *Biochim. Biophys. Acta-Biomembr.* **1995**, *1239*, 58–66.
- (35) Kano, K.; Kawazumi, H.; Ogawa, T.; Sunamoto, J. *J. Phys. Chem.* **1981**, *85*, 2204–2209.
- (36) Monteiro, J. P.; Martins, A. F.; Lúcio, M.; Reis, S.; Pinheiro, T. J. P.; Geraldes, C. F. G. C.; Oliveira, P. J.; Jurado, A. S. *Toxicol. Vitro* **2011** article in press.
- (37) Grancelli, A.; Morros, A.; Cabanas, M. E.; Domenech, O.; Merino, S.; Vazquez, J. L.; Montero, M. T.; Vinas, M.; Hernandez-Borrell, J. *Langmuir* **2002**, *18*, 9177–9182.
- (38) Schmidt, T. F.; Caseli, L.; Nobre, T. M.; Zaniquelli, M. E. D.; Oliveira, O. N. *Colloids Surf. A* **2008**, *321*, 206–210.
- (39) Wang, Z. N.; Yang, S. H. *ChemPhysChem* **2009**, *10*, 2284–2289.
- (40) Sabatini, K.; Mattila, J. P.; Megli, F. M.; Kinnunen, P. K. J. *Biophys. J.* **2006**, *90*, 4488–4499.
- (41) Shen, Y. H.; Tang, Y. F.; Xie, A. J.; Zhu, J. M.; Li, S. K.; Zhang, Y. *Appl. Surf. Sci.* **2006**, *252*, 5861–5867.
- (42) Manrique-Moreno, M.; Garidel, P.; Suwalsky, M.; Howe, J.; Brandenburg, K. *Biochim. Biophys. Acta* **2009**, *1788*, 1296–1303.
- (43) Mendelsohn, R.; Mao, G. R.; Flach, C. R. *Biochim. Biophys. Acta-Biomembr.* **2010**, *1798*, 788–800.
- (44) Lorite, G. S.; Nobre, T. M.; Zaniquelli, M. E. D.; de Paula, E.; Cotta, M. A. *Biophys. Chem.* **2009**, *139*, 75–83.
- (45) Takizawa, M.; Kim, Y. H.; Urisu, T. *Chem. Phys. Lett.* **2004**, *385*, 220–224.
- (46) Tokumasu, F.; Jin, A. J.; Dvorak, J. A. *J. Electron Microsc.* **2002**, *S1*, 1–9.